www.czasopisma.pan.pl PAN POLSKA AKADEMIA NAUK www.journals.pan.pl

PAN ARCHIVES OF ACOUSTICS
Vol. **45**, No. 3, pp. 557–562 (2020)
DOI: 10.24425/aoa.2020.134071

Technical Note

Attenuation Characteristics of Vibration in a Locally Resonant Phononic Crystal Frame Structure

Yukun WANG[(1)], Denghui QIAN[(2)*], Jinghong WU[(2)], Feiyang HE[(3)]

[(1)] *State Grid Wuhu Power Supply Company*
Wuhu 241000, Anhui, China

[(2)] *Jiangsu Province Key Laboratory of Structure Engineering*
College of Civil Engineering, Suzhou University of Science and Technology
Suzhou 215011, Jiangsu, China
*Corresponding Author e-mail: dhqian@usts.edu.cn

[(3)] *Nanjing Normal University Zhongbei College*
Zhenjiang 212300, Jiangsu, China

(*received July 22, 2019; accepted April 1, 2020*)

In this paper, a frame structure based on the locally resonant (LR) mechanism of phononic crystals (PCs) is designed on account of the wide application of frame structures in high-rise buildings, and the band structures, displacement fields of eigenmodes, and transmission power spectrums of corresponding finite structure are calculated by finite element (FE) method. Numerical results and further analysis demonstrate that a full band gap with low starting frequency can be opened by the frame structure formed by periodically combining soft and hard materials, and the starting frequency can be further lowered with the adjustment of corresponding geometric parameters, which provides a theoretical basis for the studies on vibration insulation and noise reduction of high-rise buildings.

Keywords: LRPC frame structure; high-rise building; finite element method; vibration insulation and noise reduction

1. Introduction

With the development of society and technology, a large number of high-rise and even super-tall buildings are constantly emerging. The construction of high-rise buildings is large in scale, high in engineering investment, and has multiple purpose integrating shopping malls, hotels, offices, and so on. The number of people in its interior is huge, and it is generally an iconic building in the city with important symbolic significance and great social influence. In order to ensure the safety of high-rise buildings, it is necessary to consider the vibration control of the structure under external loads such as earthquakes and wind loads (Ramezani *et al.*, 2018; Hu *et al.*, 2018). In addition, with the tremendous development of industry and transportation, the problems of vibration and noise pollution attract more and more attention. For high-rise edifices such as hotels and office buildings that need quiet surrounding, vibration and noise isolation are also taken into consideration (Vladimirovich *et al.*, 2014). If the vibration source or noise source is given, vibration and noise control is often performed from the propagation path. Because frame structures have a wide range of applications in high-rise buildings, research on the vibration control along with them will inevitably promote the realisation of vibration insulation and noise reduction.

The concept of PCs has opened up a new research direction for theoretical research and structural design of structural vibration insulation and noise reduction, which are a kind of periodic composite structures with elastic band gaps (Wagner *et al.*, 2016; Chen, Wu, 2016; Jin *et al.*, 2017; Lebon, Rizzoni, 2018). Vibrations with the frequencies located in the region of band gaps cannot be propagated along the structures, so PCs have broad application prospects in the field of vibration insulation and noise reduction. In the research on formation mechanisms of band gaps, two types are singled out: Bragg scattering (Zhang *et al.*, 2003; Dong *et al.*, 2017) and local resonance (Liu *et al.*, 2000; Li *et al.*, 2018). The wavelength cor-

responding to the frequency in the band gap of the former is in the same order of magnitude as the lattice constant, but that of the latter is much larger than the lattice constant (Liu *et al.*, 2000). Therefore, PCs designed by the locally resonant mechanism can generate band gaps at lower frequencies than the Bragg scattering mechanism.

In recent years, PCs have been widely used in the studies on basic elastic structures. Based on the theory of PCs, the basic elastic structures were designed as periodic structures, and the corresponding elastic wave propagation characteristics were also studied. During the process of studying, two different structural design ideas were formed: filled in and stubbed on structures (Ma *et al.*, 2014). Based on the locally resonant mechanism of PCs, two component (Hsu, Wu, 2007) and three component (Xiao *et al.*, 2008) filled in single plate structures were investigated respectively. The research results show that a complete band gap can be obtained in the low frequency domain, and the band gap can be controlled by adjusting the geometric parameters. Oudich *et al.* (2010) studied the band gap properties of two component and three component stubbed on PC single plates constructed by periodically attaching rubber stubs without and with Pb capped on the surface of base plate, and results show that the extremely low frequency band gap is opened by the coupling between localised mode in the stub and Lamb mode in the plate. The propagation properties of flexural waves in the simplified model of composite LRPC single plate were investigated by Qian and Shi (2017) who combined and simplified both filled in and stubbed on structures.

In summary, if the design idea of traditional PC is introduced into frame structures, it will have an important theoretical significance and application value for the design of vibration reduction and noise reduction for high-rise buildings. Based on the design ideas of filled in PC single plate structures, the soft and hard materials are combined to form a resonant unit, and a corresponding LRPC frame structure is constructed. The band gap characteristics of such a structure are studied by calculating the band structures, displacement fields of eigenmodes, and transmission power spectrums of the corresponding finite structure. In addition, the influence rules of geometric parameters on band gaps are studied.

2. Model and method

As shown in Fig. 1a, the LRPC frame structure is composed of hard and soft materials periodically. The main part of structure is made of iron material (labeled by blue), which is periodically replaced and filled with rubber material (labeled by grey). The unit cell is shown in Fig. 1b, where b is the side length, d is the thickness, h is the height of the frame structure. Particularly, lattice constant $a = b$ because the unit cell is square, and the length of rubber on each side of the unit cell is $(b - 2d)/2$. In addition, the mass density, elasticity modulus and Poisson's ratio of iron and rubber are given in Table 1.

Finite element method (FEM) is applied to calculate the band structure of the proposed frame, and commercial software COMSOL Multiphysics is adopted to help implementation. On account of the infinite periodicity of PC structure in x and y directions, only the unit cell is needed to be taken into consideration and the periodic boundary condition is applied to the interfaces between the nearest unit cells (Oudich *et al.*, 2010; Qian, Shi, 2017),

$$u_i(x+a, y+a) = u_i(x, y)e^{-\mathrm{i}(k_x a + k_y a)}, \quad (i = x, y, z). \tag{1}$$

Here, if i equals to x, y, and z, u_i represents the components of three dimensional displacement field $\mathbf{u}$ along x-direction, y-direction, and z-direction, respectively. Besides, k_x and k_y are the components of Bloch wave vector $\mathbf{k}$ limited in the irreducible first Brillouin zone (1BZ).

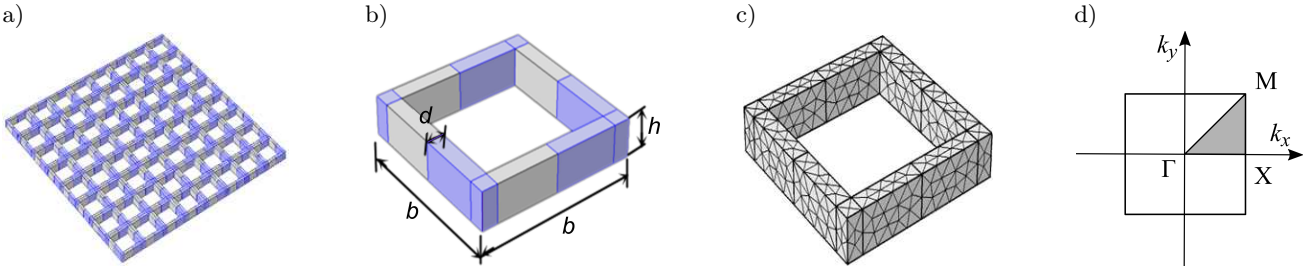

Fig. 1. a) Model of LRPC frame structure, b) its unit cell, c) meshing of the unit cell, d) and the irreducible first Brillouin zone (1BZ).

Table 1. Materials' parameters used in calculations.

Material	Mass density [kg/m^3]	Young's modulus [10^{10} N/m^2]	Poission's ratio
Iron	7780	21.06	0.3
Rubber	1300	1.175e–5	0.469

The stress free boundary condition is applied to all the other surfaces except for the interfaces. In addition, the default tetrahedral mesh provided by the software is used during meshing the unit cell.

By substituting periodic boundary condition (Eq. (1)) to free vibration characteristic equation of FEM, it gives:

$$\left(\mathbf{K} - \omega^2 \mathbf{M}\right)\mathbf{u} = \mathbf{0}. \tag{2}$$

Here, what should be noted is that the elements in stiffness matrix $\mathbf{K}$ and mass matrix $\mathbf{M}$ are coupled with the items containing Bloch wave vector $\mathbf{k}$, such as $e^{-ik_x a}$, $e^{-ik_y a}$, $e^{-i(k_x a + k_y a)}$ and so on. They are not the original structural stiffness and mass matrices of classical FEM anymore.

As shown in Eq. (2), it's a typical generalised eigenvalue problem for ω^2. A series of eigen frequencies can be received by solving the equation for each given Bloch wave vector $\mathbf{k}$. Finally, the band structure of LRPC frame structure can be obtained by scanning all $\mathbf{k}$ in the irreducible first Brillouin zone (1BZ).

In addition, the transmission power spectrum of corresponding finite frame structure is calculated by:

$$T = 20 \times \log_{10}\left|\frac{u_{\text{out}}}{u_{\text{in}}}\right|, \tag{3}$$

where T represents the transmission coefficient of vibration, u_{in} and u_{out} denote the input and output displacements, respectively.

3. Numerical results and analyses

3.1. Band structures, eigenmodes, and transmission power spectrums

Figure 2 shows the band structure of LRPC frame structure, transmission power spectrums of longitudinal vibration, and flexural vibration of corresponding finite 8×8 system, respectively. During the calculations, all the materials' parameters are shown in Table 1, and the geometric parameters are as follows: $a = b = 0.2$ m, $d = 0.02$ m and $h = 0.04$ m. Besides, during the calculation of transmission power spectrums, the excitation point is picked on one end of the frame structure as well as the response point is picked on the other end of the structure, as shown in Fig. 3. From Fig. 2a, it can be found that there are two band gaps in band structure under 53 Hz, from which the first one is between 11.5 Hz and 26.4 Hz, and the second one is between 31.5 Hz and 51.2 Hz. By comparing the attenuation frequency ranges of transmission power spectrums of longitudinal and flexural vibrations with the band gap frequency range of the band structure, it can be found that the frequency ranges basically match. The results prove again that the band gap frequency region of infinite PC structure coincides with the vibration attenuation frequency region of corresponding finite structure (Ma *et al.*, 2014; Hsu, Wu, 2007; Xiao *et al.*, 2008).

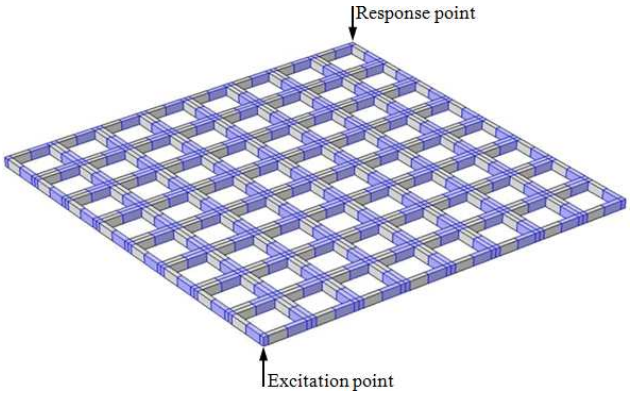

Fig. 3. Meshing of the finite LRPC frame structure made of 8×8 unit cells.

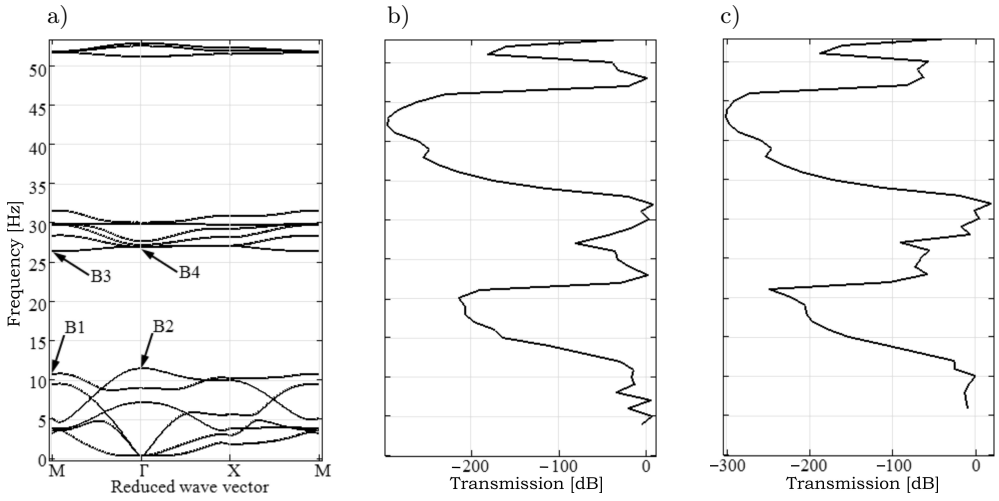

Fig. 2. Band structure of the frame structure and transmission power spectrums of the corresponding finite 8×8 system: a) band structure, b) transmission power spectrum of longitudinal vibration, and c) transmission power spectrum of flexural vibration.

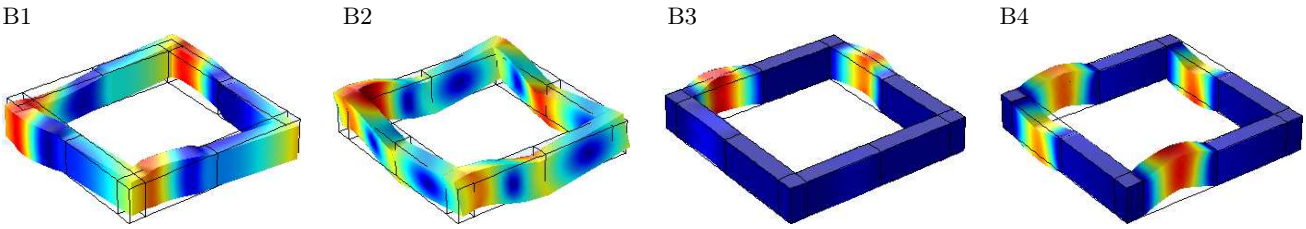

Fig. 4. Displacement fields of eigenmodes labelled in Fig. 2a.

To better analyse the band gap characteristics of LRPC frame structure, four displacement fields of eigenmodes (labelled by B1-B4 shown in Fig. 2a) are displayed in Fig. 4. For the first two modes, the whole structure is vibrated and the main vibration is concentrated on the material rubber. But for the last two figures, only the rubber vibrates. Besides, modes B1 and B3 can be regarded as a couple whose vibration is along the longitudinal direction, while modes B2 and B4 can be treated as the couple with flexural vibration. Moreover, "base-spring-mass" simplified model can be applied to help understand the vibrations of modes B3 and B4 whose hard iron material is equivalent to the base and soft rubber material is equivalent to the spring and mass.

Figure 5 displays the vibration modes of the corresponding 8×8 finite frame structure whose frequencies fall in the frequency ranges of band gaps. The calculation model is also shown in Fig. 3, and a specified displacement field is applied at the excitation point. Two frequencies, f = 20 Hz and f = 40 Hz, are picked inside the first and second band gap, respectively. By comparing Figs 5a and 5b, it can be found that vibrations only appear near the excitation point and cannot be propagated along the frame structure, from which it can be concluded that the LRPC frame structure can reliably restrain the propagation of vibration.

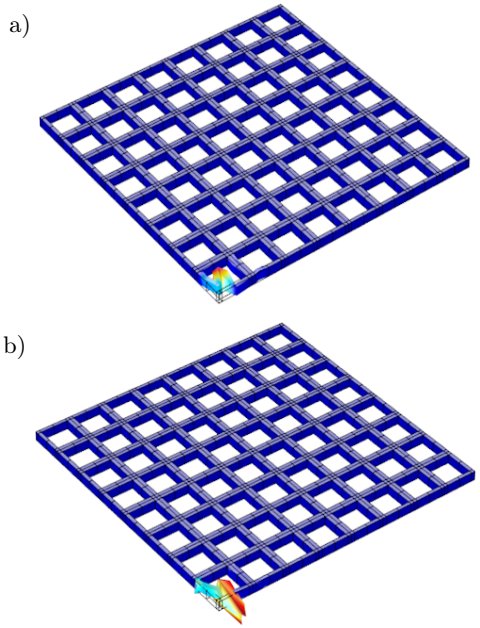

Fig. 5. Vibration modes corresponding to the frequency: a) f = 20 Hz and b) f = 40 Hz located inside the frequency ranges of band gaps.

3.2. Influence of geometric parameters on the band gap

In this section, side length b, thickness d, and height h are picked to analyse the influence rules of geometrical parameters on the first band gap, which is represented by the starting frequency f_s (larger value between f_1 and f_2), ending frequency f_e (smaller value between f_3 and f_4), and band gap width f_w (difference between f_e and f_s). During the calculation, all the parameters except for the influencing one are the same as those in the example from Fig. 2a.

Figure 6 shows the influence of side length b on the first band gap. Here, b is from 0.2 m to 0.4 m. As shown in the figure, with the increase of b, all the frequencies f_1, f_2, f_3, and f_4 keep decreasing. Simplified model "base-spring-mass" can be applied to explain the phenomenon qualitatively. For modes B3 and B4, with the increase of b, the equivalent mass increases and the equivalent spring stiffness decreases, which leads the equivalent frequency decreases. For modes B1 and B2, a critical side length b = 0.23 m exists. If b < 0.23 m, the starting frequency $f_s = f_2$, or else

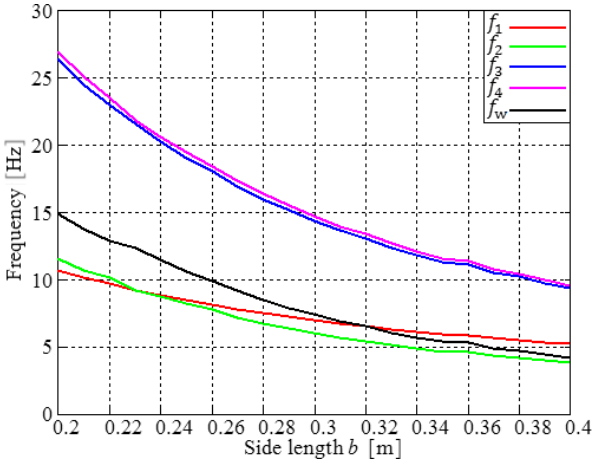

Fig. 6. Influence of side length b on first band gap.

$f_s = f_1$. Because the downtrend of f_e is larger than f_s, the band gap width f_w also keeps decreasing with the increase of the side length.

Figure 7 displays the influence of thickness d on the first band gap. Here, d is from 0.01 m to 0.04 m. As shown in the figure, thickness d has very little impact on f_1 and f_2, which can be attributed to the fact that vibration of the whole structure involves modes B1 and B2. But with the increase of d, both f_3 and f_4 keeps increasing, which leads to band gap width f_w to increase. For modes B3 and B4, by increasing d, both the equivalent mass and spring stiffness increase, but the amplification of spring stiffness is larger than that of mass, which is the reason for the influencing rules of f_3 and f_4. For modes B3 and B4, a critical thickness $d = 0.022$ m exists. If $d < 0.022$ m, the ending frequency $f_e = f_3$, or else $f_e = f_4$.

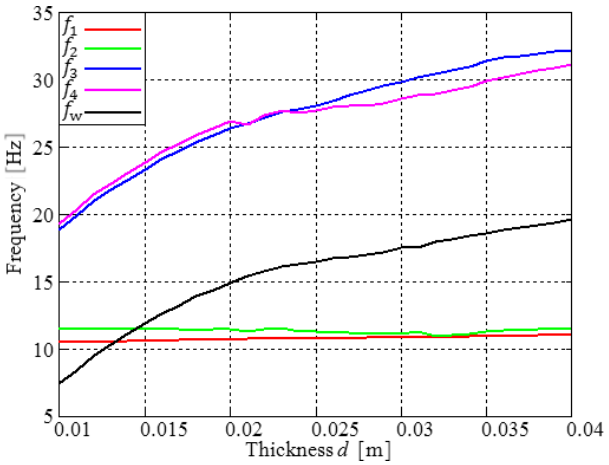

Fig. 7. Influence of thickness d on first band gap.

Figure 8 shows the influence of height h on the first band gap. Here, h is from 0.03 m to 0.06 m. As shown in the figure, all the influencing curves are tanglesome, which illustrates that height affects the first band gap irregularly. But from the overall trends, height h has little effect on f_1 and f_3. With the increase of h, both f_2 and f_4 increase, which can be attributed to the fact that both the equivalent mass and spring stiffness increase. In addition, two critical heights $h = 0.035$ m and $h = 0.037$ m appear. If $h < 0.035$ m, the starting frequency $f_s = f_1$, or else $f_s = f_2$. If $h < 0.037$ m, the ending frequency $f_e = f_4$, or else $f_e = f_3$. With the combined action of f_1, f_2, f_3, and f_4, band gap width f_w increases firstly, then decreases, and lastly keeps stable.

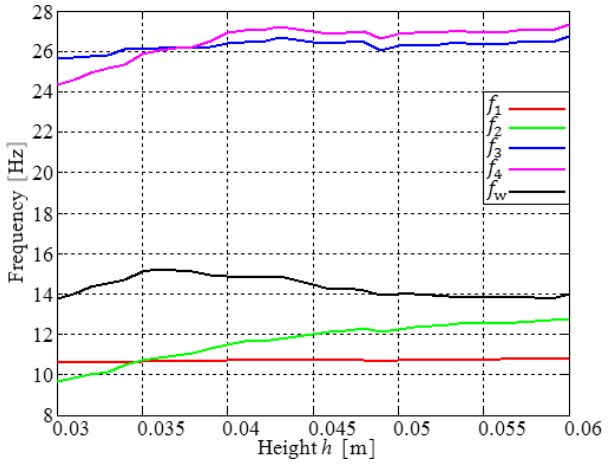

Fig. 8. Influence of height h on the first band gap.

4. Conclusions

In this paper, the band structure of proposed LRPC frame, the displacement fields, and transmission curves of relevant finite structure are calculated by FE method. The band gap characteristics of such a structure are analysed in detail. The main conclusions are as follows:

1) Complete band gaps in the low frequency regions are opened in the band of LRPC frame structure constructed by periodically repeating hard iron material and soft rubber material. Besides, the band gap frequency range basically matches the attenuation frequency region of a corresponding finite structure. For the formation of the first band gap, it can be regarded as the combined action of longitudinal and flexural vibration.

2) With the increase of side length, all the starting frequency, ending frequency, and band gap width keep decreasing. With the increase of thickness, the ending frequency and band gap width keep increasing but with the starting frequency almost unchanged. Height affects the first band gap irregularly. But from the overall trends, with the increase of height, the starting frequency keeps stable firstly and then increases, the ending frequency increases firstly and then keeps almost stable, which leads to the band gap width firstly increasing, then decreasing and lastly remaining stable.

All the work provides a theoretical basis for the studies on vibration insulation and noise reduction of frame structures, which will play an active role in the control of vibration and noise in high-rise buildings.

Acknowledgments

This research was supported by the National Natural Science Foundation of China (Nos. 11847009 and 41907232), the Natural Science Foundation of Suzhou University of Science and Technology (No. XKQ2018007) and a Project Funded by the Priority Academic Program Development of Jiangsu Higher Education Institutions.

References

1. Chen Z.G., Wu Y. (2016), Tunable topological phononic crystals, *Physical Review Applied*, **5**(5): 054021, doi: 10.1103/PhysRevApplied.5.054021.
2. Dong Y., Yao H., Du J., Zhao J., Jiang J. (2017), Research on local resonance and Bragg scattering coexistence in phononic crystal, *Modern Physics Letters B*, **31**(11): 1750127, doi: 10.1142/S0217984917501275.
3. Hsu J.C., Wu T.T. (2007), Lamb waves in binary locally resonant phononic plates with two-dimensional lattices, *Applied Physics Letters*, **90**(20): 201904, doi: 10.1063/1.2739369.
4. Hu R., Xu Y., Lu X., Zhang C., Zhang Q., Ding J. (2018), Integrated multi-type sensor placement and response reconstruction method for high-rise buildings under unknown seismic loading, *Structural Design of Tall & Special Buildings*, **27**(6): 1453, doi: 10.1002/tal.1453.
5. Jin Y., Pennec Y., Pan Y., Djafari-Rouhani B. (2017), Phononic crystal plate with hollow pillars connected by thin bars, *Journal of Physics D: Applied Physics*, **50**(3): 035301, doi: 10.1088/1361-6463/50/3/035301.
6. Lebon F., Rizzoni R. (2018), Higher order interfacial effects for elastic waves in one dimensional phononic crystals via the Lagrange-Hamilton's principle, *European Journal of Mechanics-A/Solids*, **67**: 58–70, doi: 10.1016/j.euromechsol.2017.08.014.
7. Li S., Dou Y., Chen T., Wan Z., Guan Z. (2018), A novel metal-matrix phononic crystal with a low-frequency, broad and complete, locally-resonant band gap, *Modern Physics Letters B*, **32**(19): 1850221, doi: 10.1142/S0217984918502214.
8. Liu Z. *et al.* (2000), Locally resonant sonic materials, *Science*, **289**(5485): 1734–1736, doi: 10.1126/science.289.5485.1734.
9. Ma J., Hou Z., Assouar B.M. (2014), Opening a large full phononic band gap in thin elastic plate with resonant units, *Journal of Applied Physics*, **115**(9): 093508-1–5, doi: 10.1063/1.4867617.
10. Oudich M., Li Y., Assouar B.M., Hou Z. (2010), A sonic band gap based on the locally resonant phononic plates with stubs, *New Journal of Physics*, **12**(8): 083049, doi: 10.1088/1367-2630/12/8/083049.
11. Qian D., Shi Z. (2017), Bandgap properties in simplified model of composite locally resonant phononic crystal plate, *Physics Letters A*, **381**(40): 3505–3513, doi: 10.1016/j.physleta.2017.08.058.
12. Ramezani M., Bathaei A., Ghorbani-Tanha A.K. (2018), Application of artificial neural networks in optimal tuning of tuned mass dampers implemented in high-rise buildings subjected to wind load, *Earthquake Engineering and Engineering Vibration*, **17**(4): 903–915, doi: 10.1007/s11803-018-0483-4.
13. Vladimirovich D.A., Aleksandrovich T.V., Petrovich G.O. (2014), Research on noise in hotel rooms, *World Applied Sciences Journal*, **30**(MCTT): 87–88, http://www.idosi.org/wasj/wasj30(mett)14/34.pdf.
14. Wagner M.R. *et al.* (2016), Two-dimensional phononic crystals: disorder matters, *Nano Letters*, **16**(9): 5661, doi: 10.1021/acs.nanolett.6b02305.
15. Xiao W., Zeng G.W., Cheng Y.S. (2008), Flexural vibration band gaps in a thin plate containing a periodic array of hemmed discs, *Applied Acoustics*, **69**(3): 255–261, doi: 10.1016/j.apacoust.2006.09.003.
16. Zhang X., Liu Z., Liu Y., Wu F. (2003), Elastic wave band gaps for three-dimensional phononic crystals with two structural units, *Physics Letters A*, **313**(5–6): 455–460, doi: 10.1016/s0375-9601(03)00807-7.